Inorg. Chem. **2008**, *47*, 1370−1381

Facile Synthesis and Relaxation Properties of Novel Bispolyazamacrocyclic Gd^{3+} Complexes: An Attempt towards Calcium-Sensitive MRI Contrast Agents

Anurag Mishra,[†] Petra Fousková,[‡] Goran Angelovski,[†] Edina Balogh,[§] Anil K. Mishra,[⊥] Nikos K. Logothetis,*[,†,||] and Éva Tóth*[,‡]

Department Physiology of Cognitive Processes, MPI for Biological Cybernetics, 72076 Tübingen, Germany, Centre de Biophysique Moléculaire, CNRS, rue Charles Sadron, 45071 Orléans Cedex 2, France, Institut des Sciences et Ingénierie Chimiques, Ecole Polytechnique Fédérale de Lausanne, CH-1015 Lausanne, Switzerland, Imaging Science and Biomedical Engineering, University of Manchester, Manchester, United Kingdom, and Division of Cyclotron and Radiopharmaceutical Sciences, INMAS, Timarpur, Delhi 110054, India

Received September 5, 2007

Three novel GdDO3A-type bismacrocyclic complexes, conjugated to Ca^{2+} chelating moieties like ethylenediaminetetraacetic acid and diethylenetriamine pentaacetic acid bisamides, were synthesized as potential "smart" magnetic resonance imaging contrast agents. Their sensitivity toward Ca^{2+} was studied by relaxometric titrations. A maximum relaxivity increase of 15, 6, and 32% was observed upon Ca^{2+} binding for Gd_2L^1, Gd_2L^2, and Gd_2L^3, respectively (L^1 = *N*,*N*-bis{1-[{[({1-[1,4,7-tris(carboxymethyl)-1,4,7,10-tetraazacyclododecane-10-yl]eth-2-yl}amino)carbonyl]-methyl}-(carboxymethyl)amino]eth-2-yl}aminoacetic acid; L^2 = *N*,*N*-bis[1-({[({α-[1,4,7-tris(carboxymethyl)-1,4,7,10-tetraazacyclododecane-10-yl]-*p*-tolylamino}carbonyl)methyl]-(carboxymethyl)}amino)eth-2-yl]aminoacetic acid; L^3 = 1,2-bis[{[({1-[1,4,7-tris(carboxymethyl)-1,4,7,10-tetraazacyclododecane-10-yl]eth-2-yl}amino)carbonyl]methyl}-(carboxymethyl)amino]ethane). The apparent association constants are log $K_A = 3.6 \pm 0.1$ for Gd_2L^1 and log $K_A = 3.4 \pm 0.1$ for Gd_2L^3. For the interaction between Mg^{2+} and Gd_2L^1, log $K_A = 2.7 \pm 0.1$ has been determined, while no relaxivity change was detected with Gd_2L^3. Luminescence lifetime measurements on the Eu^{3+} complexes in the absence of Ca^{2+} gave hydration numbers of $q = 0.9$ (Eu_2L^1), 0.7 (Eu_2L^2), and 1.3 (Eu_2L^3). The parameters influencing proton relaxivity of the Gd^{3+} complexes were assessed by a combined nuclear magnetic relaxation dispersion (NMRD) and ^{17}O NMR study. Water exchange is relatively slow on Gd_2L^1 and Gd_2L^2 ($k_{ex}^{298} = 0.5$ and $0.8 \times 10^6\ s^{-1}$), while it is faster on Gd_2L^3 ($k_{ex}^{298} = 80 \times 10^6\ s^{-1}$); in any case, it is not sensitive to the presence of Ca^{2+}. The rotational correlation time, τ_R^{298}, differs for the three complexes and reflects their rigidity. Due to the benzene linker, the Gd_2L^2 complex is remarkably rigid, with a correspondingly high relaxivity despite the low hydration number ($r_1 = 10.2\ mM^{-1}s^{-1}$ at 60 MHz, 298 K). On the basis of all available experimental data from luminescence, ^{17}O NMR, and NMRD studies on the Eu^{3+} and Gd^{3+} complexes of L^1 and L^3 in the absence and in the presence of Ca^{2+}, we conclude that the relaxivity increase observed upon Ca^{2+} addition can be mainly ascribed to the increase in the hydration number, and, to a smaller extent, to the Ca^{2+}-induced rigidification of the complex.

Introduction

Molecular imaging using magnetic resonance (MR) techniques is a rapidly growing field in basic neuroscience and diagnostic medicine. The high spatial resolution and the undisputed capacity of differentiating soft tissues have highly contributed to the widespread use of this imaging modality.

* To whom correspondence should be addressed. E-mail: eva.jakabtoth@cnrs-orleans.fr (E.T.), nikos.logothetis@tuebingen.mpg.de (N.K.L.). Phone: 00 33 2 38 25 76 25(E.T.), 0049 7071 601 651(N.K.L.). Fax: 00 33 2 38 63 15 17 (E.T.), 00 49 7071 601 652 (N.K.L.).

[†] MPI for Biological Cybernetics.
[‡] CNRS.
[§] Ecole Polytechnique Fédérale de Lausanne.
[||] University of Manchester.
[⊥] INMAS.

10.1021/ic7017456 CCC: $40.75
Published on Web 01/01/2008

Magnetic resonance imaging (MRI) offers the potential of realistic three-dimensional imaging of biological structures, where the signal is based upon the resonance of water protons.[1] Gadolinium(III)-based MR contrast agents are commonly applied to increase the relaxation rates of the surrounding water protons, which makes them appear as a bright spot of amplified intensity in T_1-weighted images.[2–4] The markedly enhanced contrast of the images and the improved sensitivity are of extensive assistance in clinical and experimental settings.

The development of exogenous "smart" contrast agents (SCAs) is a step further in the efforts to improve the specificity of *in vivo* MR imaging. Ideally, SCAs cage Gd^{3+} within the delivery molecule, shielding it from water protons and rendering it silent until the intended trigger opens the cage door. The modulation of the relaxivity of the SCAs can be achieved by specific physiological or biochemical triggers such as changes in pH,[5–9] metal ion concentration,[10–15] enzymatic activity,[16,17] oxygen activation,[18] and neurotransmitter concentration or by binding to intra- or extracellular messengers.[19]

The use of MRI to detect fluctuations in the concentration of vital metal ions has recently received much attention. The pioneering work in this area was conferred by Meade and co-workers, who focused on the important role played by intracellular calcium(II) in signal transduction.[10,20] Zinc(II) is another significant metal ion that regulates synaptic transmission and cell death. Selectively sensing Zn^{2+} ions with contrast agents had been previously discussed by

Scheme 1. Structures of the Ligands Studied

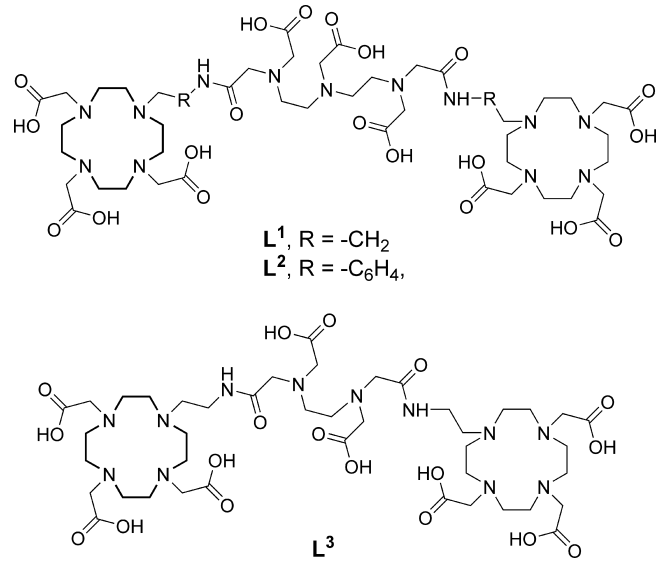

Hanaoka et al. and Trokowski et al.[12,13] Desreux et al. embarked on an innovative approach based on self-assembly toward the development of iron-activated GdDO3A-based CAs.[14] Recently, Que and Chang introduced a copper(II)-sensitive SCA.[15]

Revealing the role of Ca^{2+} in neural signaling is a hot field in neuroscience research. The extracellular concentrations of Ca^{2+} and Mg^{2+} play an important role in both physiological and pathological processes in the nervous system. Significant fluctuations in their concentrations occur in association with normal brain activity, as well as with a variety of pathological phenomena including ischemia, hypoglycemia, and seizures.[21,22] Intracellular Ca^{2+} has an important role in muscular contraction, neural transduction, and hormonal secretion.[23] Changes in the cytosolic concentration of Ca^{2+} trigger changes in cellular metabolism and are responsible for cell signaling and regulation.[11] The development of selective fluorescent reporter molecules has helped in the understanding of multiple roles of calcium.[24]

For the detection of neuronal activity by MRI, the central challenge lies in translating the activity into changes in MR image contrast. In an effort toward this objective, we designed Gd^{3+}-based systems whose relaxivity is potentially influenced by the variations of Ca^{2+} concentration in the physiological range, in particular in the extracellular space. We report here the facile synthesis and physicochemical characterization of three novel bismacrocyclic Gd^{3+} complexes, derived from DO3A-ethylamine (DO3A-EA) or *p*-aminobenzyl-DO3A (pABn-DO3A) (Scheme 1). The fundamental in the design of L^1, L^2, and L^3 is to keep the coordination properties of DO3A-type ligands for Ln^{3+}. The macrocycle contains three carboxylate groups and four nitrogens from the cyclen ring to form a stable complex with Ln^{3+}. The fourth nitrogen is appended with a potentially reactive group (aryl/alkyl amine) where anhydrates of

(1) Rudin, M. *Anal. Bioanal. Chem.* **2003**, *377*, 955.
(2) Lauffer, R. B. *Chem. Rev.* **1987**, *87*, 901.
(3) Caravan, P.; Ellison, J. J.; McMurry, T. J.; Lauffer, R. B *Chem. Rev.* **1999**, *99*, 2293.
(4) Merbach, A. E.; Tóth, E. *The chemistry of contrast agents in medical magnetic resonance imaging*; Wiley: Chichester, U.K., 2001.
(5) Zhang, S.; Wu, K.; Sherry, A. D. *Angew. Chem., Int. Ed.* **1999**, *38*, 3192.
(6) Aime, S.; Crich, S. G.; Botta, M.; Castellano, G.; Gianolio, E.; Pagliarin, R. *Chem. Commun.* **1999**, 1577.
(7) Lowe, M. P.; Parker, D.; Reany, O.; Aime, S.; Botta, M.; Castellano, G.; Gianolio, E.; Pagliarin, R. *J. Am. Chem. Soc.* **2001**, *123*, 7601.
(8) Aime, S.; Castelli, D. D.; Terreno, E. *Angew. Chem., Int. Ed.* **2002**, *41*, 4334.
(9) Hovland, R.; Glogard, C.; Aasen, A. J.; Klaveness, J. *J. Chem. Soc., Perkin Trans.* **2001**, *2*, 929.
(10) Li, W.-H.; Fraser, S. E.; Meade, T. J. *J. Am. Chem. Soc.* **1999**, *121*, 1413.
(11) Atanasijevic, T.; Shusteff, M.; Fam, P.; Jasanoff, A. *Proc. Natl. Acad. Sci. U.S.A.* **2006**, *103*, 14707.
(12) Hanaoka, k.; Kikuchi, Y.; Urano, Y.; Nagano, T. *J. Chem. Soc., Perkin Trans.* **2001**, *2*, 1840.
(13) Trokowski, R.; Ren., J.; Kalman, F. K.; Sherry, A. D. *Angew. Chem., Int. Ed.* **2005**, *44*, 6920.
(14) Comblin, V.; Gilsoul, D.; Hermann, M.; Humbelt, V.; Jacques, V.; Mesbahi, M.; Sauvage, C.; Desreux, J. F. *Coord. Chem. Rev.* **1999**, *185–186*, 451.
(15) Que, E. L.; Chang, C. J. *J. Am. Chem. Soc.* **2006**, *128*, 15942.
(16) Moats, R. A.; Fraser, S. E.; Meade, T. J. *Angew Chem., Int. Ed.* **1997**, *36*, 726.
(17) Louie, A. Y.; Huber, M. M.; Ahrens, E. T.; Rothbacher, U.; Moats, R. A.; Jacobs, R. E.; Fraser, S. E.; Meade, T. J. *Nat. Biotechnol.* **2000**, *18*, 321.
(18) Aime, S.; Botta, M.; Gianolio, E.; Terreno, E. *Angew Chem., Int. Ed.* **2000**, *39*, 747.
(19) Bulte, J. W. M.; Bryant, L. H. *Molecular and Cellular Magnetic Resonance Contrast Agents, in Physics and Chemistry Basis of Biotechnology*; Springer: The Netherlands, 2002; Vol. *7*, pp 191–221.
(20) Li, W.; Parigi, G.; Fragai, M.; Luchinat, C.; Meade, T. J. *Inorg. Chem.* **2002**, *41*, 4018.
(21) Massimini, M.; Amzica, F. *J. Neurophysiol.* **2001**, *85*, 1346.
(22) Silver, I. A.; Erecinska, M. *J. Gen. Physiol.* **1990**, *95*, 837.
(23) Charles, A. *GLIA* **1998**, *24*, 39.
(24) Tsien, R. Y. *Biochemistry* **1980**, *19*, 2396.

diethylenetriamine pentaacetic acid/ethylenediaminetetraacetic acid (DTPA/EDTA) are reacted to form bismacrocyclic CAs through amide bonds. The two macrocyclic units hold a lanthanide ion each, while the EDTA-bisamide/DTPA-bisamide constitutes the calcium-sensitive core. We specifically aim at sensing the variation of Ca^{2+} concentration in the extracellular space, which is in the millimolar range. The common fluorescent Ca^{2+} indicators used in biological applications and based on $BAPTA^{4-}$ are adapted to assess the cytosolic free Ca^{2+} concentration in the micromolar range (H_4BAPTA = 1,2-bis(*o*-aminophenoxy)ethane-N,N,N′,N′-tetraacetic acid). The relaxivity response of a probe with a Ca^{2+}affinity of $K \sim 10^6$ M such as that of $BAPTA^{4-}$ would be already leveled off at the millimolar level. Therefore, the Ca^{2+} binding moiety in the central part of our ligands was designed to have a reduced affinity toward Ca^{2+} in order to shift to higher Ca^{2+} concentrations the range where the probe is expected to have a relaxivity response.

The proton relaxivities of the Gd^{3+} complexes were studied at variable Ca^{2+} concentrations by relaxometric titrations. In the objective of relating the Ca^{2+}-dependent relaxivity response to the microscopic parameters of the Gd^{3+} chelate, we carried out a detailed mechanistic study. We used UV–vis absorbance and luminescence lifetime measurements on the corresponding Eu^{3+} complexes to assess the hydration state and its variation on Ca^{2+} addition. The Gd^{3+} complexes with L^1–L^3 have been characterized by variable-temperature ^{17}O NMR spectroscopy and variable-field relaxivity measurements (nuclear magnetic relaxation dispersion, NMRD) which allowed us to calculate the parameters describing water exchange and rotational dynamics.

Experimental Section

Materials and Methods. All reagents and solvents were used at the purest commercially available grade without further purification. Cyclen was purchased from Strem, France. Bromoacetonitrile, *tert*-butylbromoacetate, Raney-nickel (Ra-Ni), Pd/C (10%), trifluoroacetic acid (TFA), EDTA-bisanhydride, DTPA-bisanhydride and N,N-dimethylformamide (DMF extra dry), were purchased from Aldrich, Germany. Dichloromethane and analytical and HPLC grade methanol (MeOH) were purchased from Acros Organics, Germany. Sodium carbonate, acetonitrile (MeCN, anhydrous), gadolinium chloride hexahydrate, europium chloride hexahydrate, hydrogen chloride, silica gel 60 (70–230 mesh), sodium hydroxide, sodium sulfate, and potassium carbonate were purchased from Fluka, Germany. Pure water (18 MΩ cm^{-1}) was used throughout.

Reversed-phase high-performance liquid chromatography (RP-HPLC) was performed at room temperature on a Varian PrepStar Instrument, Australia, equipped with PrepStar SD-1 pump heads. UV absorbance was measured using a ProStar 335 photodiode array detector at 214 and 254 nm. Analytical RP-HPLC was performed in a stainless steel Chromsep (length 250 mm, internal diameter 4.6 mm, outside diameter 3/8 in., and particle size 8 μm) C_{18} column, and preparative RP-HPLC was performed in a stainless steel Chromsep (length 250 mm, internal diameter 41.4 mm, outside diameter 2 in., and particle size 8 μm) C_{18} column (Varian, Advanced Chromatographic Solutions). The compounds were purified using one of the two methods. In method A, the gradient was used with the mobile phase starting from 95% solvent A (water) and 5% solvent B (MeOH), moving to 80% B in 10 min, 100% B in 18 min, 100% B isocratic up to 28 min, and decreasing to 5% B in 30 min. Alternatively, in method B, the gradient was used with the mobile phase starting from 5% of solvent B (MeOH) to 80% B in 15 min and decreasing to 5% B in 18 min. The flow rate generally used for analytical HPLC was 1 mL/min and for preparative HPLC was 41 mL/min. All the solvents for HPLC were filtered through a nylon-66 Millipore filter (0.45μm) and sonicated prior to use.

Thin-layer chromatography (TLC) was run on aluminum sheet silica gel plates with 0.2-mm-thick silica gel 60 F_{254} (E. Merck, Germany) using different mobile phases. The TLC plate was developed in an iodine chamber.

Analytical ^1H and ^{13}C NMR spectra were recorded on a Bruker 250 MHz spectrometer at 5.9 T (^1H; internal reference $CDCl_3$ at 7.27 ppm or D_2O at 4.75 ppm); 62.9 MHz (^{13}C; internal reference $CDCl_3$ at 77.0 ppm or TMS at 0 ppm). All experiments were performed at 25 °C.

^1H relaxometric titrations were performed on a Bruker Avance 500 spectrometer (11.75 T, 500 MHz) at 25 °C. The pH was maintained by a 0.1 M KMOPS buffer, and solutions of $CaCl_2$ and $MgCl_2$ were used for the titrations.

Electrospray ionization mass spectrometry (ESI-MS) spectra were performed on an SL 1100 system (Agilent, Germany) with ion-trap detection in the positive and negative ion modes.

UV–vis spectra of the europium(III) complexes of L^1, L^2, and L^3 were obtained on a Perkin-Elmer Lambda 19 spectrometer, in thermostatizable cells with a 10 cm optical length (λ = 577.0–581.5 nm) with data steps of 0.05 nm. The sample concentrations were about 0.01 M, and the temperature dependence was measured in a large temperature range (typically between 280 and 360 K). The technique has been described in detail in previous publications.[25]

The luminescence measurements were performed on a Varian eclipse spectrofluorimeter, equipped with a 450 W xenon arc lamp, a microsecond flash lamp, and a red-sensitive photomultiplier (300–850 nm). The luminescence spectra were obtained after excitation at the $^5L_6 \leftarrow {}^7F_0$ band (394 nm). All measurements were carried out in solutions containing 5 mM Eu^{3+} complexes of L^1, L^2, and L^3 in a 30 mM KMOPS buffer (pH 7.20) at 25 °C. The luminescence decay was recorded in the short phosphorescence lifetime mode and was repeated at least five times under each condition. The luminescence lifetime was calculated from the monoexponential fitting of the average decay data.

The ^1H NMRD profiles were recorded at the Laboratory of Inorganic and Bioinorganic Chemistry, Ecole Polytechnique Fédérale de Lausanne, Switzerland, on a Stelar Spinmaster FFC fast-field-cycling relaxometer covering magnetic fields from 2.35×10^{-4} T to 0.47 T, which corresponds to a proton Larmor frequency range of 0.01–20 MHz. The temperature was controlled by a VTC90 temperature control unit and fixed by a gas flow. The relaxivity at higher fields was recorded using Bruker Minispecs mq30 (30 MHz), mq40 (40 MHz), and mq60 (60 MHz), and on a Bruker 4.7 T (200 MHz) cryomagnet with a Bruker Avance-200 console and on a Bruker Avance 500 spectrometer (500 MHz). The temperature was measured by a substitution technique[26] or by a preliminary calibration using methanol and ethyleneglycol standards.[27]

(25) Graeppi, N.; Powell, D. H.; Laurenczy, G.; Zékány, L.; Merbach, A. E. *Inorg. Chim. Acta* **1994**, *235*, 311.
(26) Amman, C.; Meyer, P.; Merbach, A. E. *J. Magn. Reson.* **1982**, *46*, 319.
(27) Raiford, D. S.; Fisk, C. L.; Becker, E. D. *Anal. Chem.* **1979**, *51*, 2050.

The transverse ^{17}O relaxation rates ($1/T_2$) were measured in the temperature range 277–344 K, on a Bruker Avance 500 (11.75 T, 67.8 MHz) spectrometer. The temperature was calculated according to previous calibration with ethylene glycol and methanol.[27] The samples were contained in 5 mm NMR tubes and enriched with *tert*-butanol to allow for the BMS correction.[28] The $1/T_2$-data were measured using the Carr–Purcell–Meiboom–Gill spin–echo technique. Acidified water ($HClO_4$, pH 3.8) was used as an external reference. Analysis of the ^{17}O NMR and ^1H NMRD experimental data was performed with the Visualizeur/Optimiseur programs running on a Matlab platform, version 6.5.[29]

Synthesis. [4,7-Bis-butoxycarbonylmethyl-10-(cyanomethyl)-1,4,7,10-tetraaza-cyclododec-1-yl]-acetic Acid *tert*-Butyl Ester, 2. A solution of **1** (4.0 g, 7.8 mmol) and K_2CO_3 (4.3 g, 31.2 mmol) in 40 mL of MeCN was stirred at room temperature for 1 h. Bromoacetonitrile (0.65 mL, 9.3 mmol) was added in one aliquot to the above solution, and the reaction mixture was refluxed for 8 h. The reaction was monitored by TLC. After completion, the reaction mixture was filtered through a G-4 sintered funnel; the filtrate was evaporated under reduced pressure, and the residue was purified by column chromatography (silica gel, 5% MeOH in CH_2Cl_2, $R_f = 0.55$) to give 3.36 g (78%) of **2** as brownish gum. ^1H NMR ($CDCl_3$, 250 MHz): δ 1.23 (s, 9H), 1.27 (s, 18H), 2.06–2.21 (m, 6H), 2.39–2.78 (m, 10H), 2.89 (s, 4H), 3.01 (s, 2H), 3.63 (s, 2H). ^{13}C NMR ($CDCl_3$, 62.9 MHz): δ 27.7, 27.8, 42.7, 50.1, 50.4, 50.6, 50.7, 55.8, 56.7, 82.4, 82.8, 115.2, 172.9, 173.4. ESI-MS ($\pm$) calcd $C_{28}H_{51}N_5O_6$: *m/z* 554.3 $(M+H)^+$. Found: 554.8 $(M+H)^+$.

[4,7-Bis-butoxycarbonylmethyl-10-(2-aminoethyl)-1,4,7,10-tetraaza-cyclododec-1-yl]-acetic Acid *tert*-Butyl Ester, 3. A solution of **2** (3.0 g, 5.4 mmol), Ra-Ni (1.5 g), and H_2 (50 psi) in 7N NH_3/MeOH (30 mL) was stirred at room temperature in a Parr apparatus for 6 h. The reaction was monitored by TLC. After completion, the reaction mixture was filtered through a G-4 sintered funnel; the filtrate was evaporated under reduced pressure, and the residue was purified by column chromatography (silica gel, 10% MeOH in CH_2Cl_2, $R_f = 0.45$) to give 2.17 g (72%) of **3** as an off-white solid. ^1H NMR ($CDCl_3$, 250 MHz): δ 1.38 (s, 9H), 1.40 (s, 18H), 2.17–2.75 (m, 18H), 2.84 (br s, 4H), 3.03 (s, 4H), 3.10 (s, 2H). ^{13}C NMR ($CDCl_3$, 62.9 MHz): δ 27.2, 27.3, 38.0, 48.5, 48.8, 49.1, 49.6, 52.9, 54.9, 55.1, 81.3, 81.5, 171.5, 171.9. ESI-MS ($\pm$) calcd $C_{28}H_{55}N_5O_6$: *m/z* 558.4 $(M+H)^+$. Found: 558.5 $(M+H)^+$.

General Method for the Synthesis of Compounds 6–8. The solutions of **3** (for compound **6**–**7**) and **5** (for compound **8**) (2.5 equiv) in dry DMF were added dropwise to the solution of DTPA-bisanhydride/EDTA-bisanhydride (1 equiv) in dry DMF (5 mL) at 0–5 °C for 30 min under a continuous nitrogen flow. The reaction mixtures were stirred overnight at 50 °C. The progress of reactions was monitored by ESI-MS. After completion, the solvent was evaporated under reduced pressure. The crude products were purified by preparative RP-HPLC.

5,8-Bis(carboxymethyl)-10-oxo-2-(2-oxo-2-(2-(4,7,10-tris(2-*tert*-butoxy-2-oxoethyl)-1,4,7,10-tetraazacyclododecan-1-yl)ethylamino)ethyl)-13-(4,7,10-tris(2-*tert*-butoxy-2-oxoethyl)-1,4,7,10-tetraazacyclododecan-1-yl)-2,5,8,11-tetraazatridecane-1-carboxylic Acid, 6. RP-HPLC: method A, λ = 214 nm, RT = 21 min. Yield: 1.03 g (39%) of **7** as a yellowish gum. ^1H NMR ($CDCl_3$, 250 MHz): δ 1.52 (s, 36H), 1.54 (s, 18H), 2.76–3.17 (m, 20H), 3.18–3.47 (m, 16H), 3.49–3.68 (m, 16H), 3.70–3.89 (m, 13H), 3.96 (br s, 6H), 4.14 (br s, 4H). ^{13}C NMR ($CDCl_3$, 62.9 MHz): δ 29.4, 29.5, 33.2, 47.9, 49.3, 50.0, 51.3, 51.7, 52.2, 52.9, 54.9, 56.6, 57.7, 60.1, 60.8, 81.4, 81.6, 168.8, 170.2, 170.3, 172.3, 176.2. ESI-MS ($\pm$) calcd $C_{70}H_{129}N_{13}O_{20}$: *m/z* 1470.9 $(M+H)^-$. Found: 1471.3 $(M-H)^-$.

2,2′-(4,11-Dioxo-1,14-bis(4,7,10-tris(2-*tert*-butoxy-2-oxoethyl)-1,4,7,10-tetraazacyclododecan-1-yl)-3,6,9,12-tetraazatetradecane-6,9-diyl)diacetic Acid, 7. RP-HPLC: method A, λ = 214 nm, RT = 24 min. Yield: 1.13 g (52%) of **6** as a colorless gum. ^1H NMR ($CDCl_3$, 250 MHz): δ 1.46 (s, 36H), 1.48 (s, 18H), 2.60 (br s, 4H), 2.73–2.79 (m, 18H), 3.02–3.08 (m, 7H), 3.12 (s, 4H), 3.19 (br s, 3H), 3.27–3.31 (m, 2H), 3.35 (s, 8H), 3.40 (s, 4H), 3.42 (s, 6H), 3.47 (br s, 6H), 3.54–3.61 (m, 2H), 3.66 (d, J = 5.33, 2H), 3.70 (d, J = 2.66, 2H). ^{13}C NMR ($CDCl_3$, 62.9 MHz): δ 27.6, 27.7, 33.5, 47.8, 49.3, 49.9, 50.6, 52.8, 53.7, 55.0, 55.9, 59.7, 59.9, 80.9, 81.0, 169.7, 169.9, 172.6, 175.1. ESI-MS ($\pm$) calcd $C_{66}H_{122}N_{12}O_{18}$: *m/z* 1371.9 $(M+H)^+$. Found: 1371.9 $(M+H)^+$.

2,2′-2,2′-(Carboxymethylazanediyl)bis(ethane-2,1-diyl)bis((2-oxo-2-(4-((4,7,10-tris(2-tert-butoxy-2-oxoethyl)-1,4,7,10-tetraazacyclododecan-1-yl)methyl)phenylamino)ethyl)azanediyl)diacetic Acid, 8. RP-HPLC: method A, λ = 254 nm, RT = 22 min. Yield: 1.32 g (46%) of **8** as a yellowish gum. ^1H NMR ($CDCl_3$, 250 MHz): δ 1.44 (s, 36H), 1.46 (s, 18H), 2.71–2.89 (m, 20H), 2.92–3.04 (m, 9H), 3.10 (br s, 5H), 3.20 (s, 4H), 3.28 (br s, 10H), 3.31–3.36 (m, 4H), 3.38 (s, 2H), 3.44 (s, 8H), 3.48 (s, 4H), 3.81 (br s, 2H), 4.14 (br s, 3H), 6.88–7.25 (m, 4H), 7.80–8.11 (m, 4H). ^{13}C NMR ($CDCl_3$, 62.9 MHz): δ 27.9, 28.0, 48.8, 48.9, 49.8, 50.7, 50.9, 51.7, 52.1, 52.7, 55.8, 56.2, 56.3, 61.4, 81.3, 81.4, 120.2, 122.7, 124.9, 128.9, 139.4, 169.8, 169.9, 170.3, 170.6, 175.6. ESI-MS ($\pm$) calcd $C_{80}H_{133}N_{13}O_{20}$: *m/z* 1594.9 $(M-H)^-$. Found: 1595.1 $(M-H)^-$.

General Method for the Synthesis of L^1, L^2, and L^3. Neat TFA (20 mL) was added to the previously obtained compounds **6**–**8**, and the reactions were kept at room temperature for 18 h. TFA was then evaporated, dissolved in a minimum volume of MeOH (1 mL) followed by dropwise addition of diethylether at 0–5 °C, and stirred gently for 1 h at room temperature. The compounds were precipitated, and precipitates were filtered through a G-4 sintered funnel under a continuous nitrogen flow. The precipitates were dissolved in water and neutralized by adding 1 M NaOH, and the crude products were purified by preparative RP-HPLC.

***N*,*N*-Bis{1-[{[({1-[1,4,7-tris(carboxymethyl)-1,4,7,10-tetraazacyclododecane-10-yl]eth-2-yl}amino)carbonyl]methyl}-(carboxymethyl)amino]eth-2-yl}aminoacetic Acid, L^1.** RP-HPLC: method B, λ = 214 nm, RT = 2.8 min. Yield: 0.22 g (57%) of L^1 as a white solid. ^1H NMR (D_2O, 250 MHz): δ 3.01 (br s, 8H), 3.04−3.17 (m, 16H), 3.23–3.41 (m, 18H), 3.46 (br s, 6H), 3.56 (br s, 8H), 3.62 (s, 4H), 4.08 (s, 10H). ^{13}C NMR (D_2O, 62.9 MHz): δ 32.2, 46.8, 47.7, 47.8, 49.0, 49.1, 50.2, 50.8, 51.2, 51.8, 52.2, 53.5, 54.1, 164.7, 167.2, 170.7, 171.2, 171.3. ESI-MS ($\pm$) calcd $C_{46}H_{81}N_{13}O_{20}$: *m/z* 1134.5 $(M+H)^-$. Found: 1134.8 $(M-H)^-$.

***N*,*N*-Bis[1-({[({α-[1,4,7-tris(carboxymethyl)-1,4,7,10-tetraazacyclododecane-10-yl]-*p*-tolylamino}carbonyl)methyl]-(carboxymethyl)}amino)eth-2-yl]aminoacetic Acid, L^2.** RP-HPLC: method B, λ = 254 nm, RT = 2.4 min. Yield: 0.22 g (58%) of L^2 as a white solid. ^1H NMR (D_2O, 250 MHz): δ 2.87–2.99 (m, 8H), 3.12–3.22 (m, 12H), 3.24–3.34 (m, 20H), 3.41 (t, J = 5.97, 5H), 3.54 (br s, 8H), 3.58 (s, 2H), 3.60 (s, 2H), 3.81 (br s, 4H), 7.30–7.37 (m, 4H), 7.38–7.43 (m, 2H), 7.44–7.52 (m, 2H). ^{13}C NMR (D_2O, 62.9 MHz): δ 45.9, 46.8, 48.1, 48.2, 48.6, 50.6, 53.5,

(28) Zitha-Bovens, E.; Vander Elst, L.; Muller, R. N.; van Bekkum, H.; Peters, J. A. *Eur. J. Inorg. Chem.* **2001**, 3101.

(29) (a) Yerly, F. *VISUALISEUR 2.3.4.*; Institut de Chimie Moléculaire et Biologique: Lausanne, Switzerland, 1999. (b) Yerly, F. *OPTIMISEUR 2.3.4.*; Institut de Chimie Moléculaire et Biologique: Lausanne, Switzerland, 1999.

Scheme 2. Synthesis of Ligands L^1 and L^3 [a]

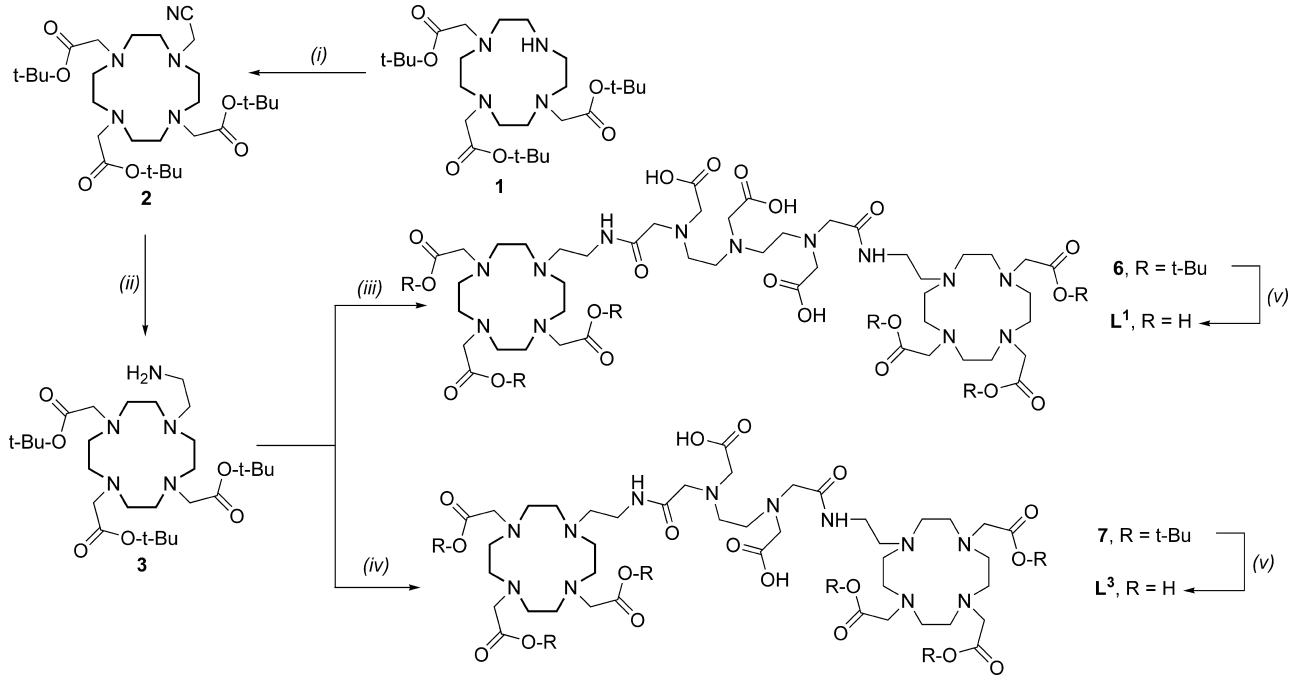

[a] Reagents and conditions: (i) bromoacetonitrile, MeCN, 78%; (ii) Ra-Ni, H_2, NH_3/MeOH (7N), 72%; (iii) DTPA-bisanhydride, DMF, 39%; (iv) EDTA-bisanhydride, DMF, 52%; (v) TFA, 55–70%.

54.2, 54.8, 56.2, 56.3, 56.9, 119.4, 121.5, 124.9, 128.1, 134.6, 168.6, 169.5, 169.8, 173.0, 175.9. ESI-MS (±) calcd $C_{56}H_{86}N_{13}O_{20}$: *m/z* 1258.6 $(M+H)^-$. Found: 1259.0 $(M-H)^-$.

1,2-Bis[{[({1-[1,4,7-tris(carboxymethyl)-1,4,7,10-tetraazacyclododecane-10-yl]eth-2-yl}amino)carbonyl]methyl}-(carboxymethyl)amino]ethane, L^3. RP-HPLC: method B, λ = 214 nm, RT = 3.4 min. Yield: 0.26 g (68%) of L^3 as an off-white solid. ^{1}H NMR (D_2O, 250 MHz): δ 2.88−2.97 (m, 4H), 2.98–3.17 (16, H), 3.21 (s, 4H), 3.24 (br s, 2H), 3.26–3.47 (m, 23H), 3.52 (s, 4H), 3.70 (br s, 8H), 3.78 (br s, 4H). ^{13}C NMR (D_2O, 62.9 MHz): δ 37.9, 50.8, 51.5, 53.0, 53.4, 53.7, 53.9, 54.2, 57.9, 59.2, 59.8, 172.3, 174.1, 176.6, 178.4. ESI-MS (±) calcd $C_{42}H_{75}N_{12}O_{18}$: *m/z* 1033.5 $(M+H)^-$. Found: 1033.6 $(M-H)^-$.

Preparation of the Ln^{3+} Complexes. The Ln^{3+} complexes of L^1, L^2, and L^3 were prepared by mixing the ligand and the $LnCl_3$ solutions in 1:2 molar ratios. The reaction mixture was stirred at 50–60 °C for 18 h. The pH was periodically adjusted to 7.0–7.5 using a solution of NaOH (1 M). After 18 h, the reaction mixture was cooled down and passed through chelex-100 at room temperature to trap the eventual free Ln^{3+}, and the Ln^{3+}-loaded complex was recovered. The absence of free Gd^{3+} was checked with xylenol orange indicator.[30] The fractions were lyophilized, and white solids were obtained. The aqueous solution samples were obtained by dissolution of these solids. For each Gd_2L sample, the Gd^{3+} concentration has been determined by measuring the bulk magnetic susceptibility shifts.[31]

Result and Discussion

Synthesis. DO3A is an eminent building block for the preparation of macrocyclic, Ln^{3+}-based imaging probes. One of the nitrogens of the macrocycle was appended with an ethylamine or *p*-aminobenzyl reactive group to form the known bifunctional precursors DO3A-EA and pABn-DO3A. They both bear an amine function that is readily reactive toward most electrophiles such as anhydrides, aldehydes, carboxylic acids, and isothiocyanates.[32–34] The trisubstituted product **1** was synthesized by the reaction of *tert*-butylbromoacetate on cyclen.[35] Alkylation on **1** with bromoacetonitrile gave cyano-containing ligand **2**, and the corresponding amine derivative **3** was obtained by the reduction of the cyano group in the presence of Ra-Ni, H_2, and 7N NH_3/MeOH by using a Parr apparatus at room temperature.[36,37] After the successful synthesis of precursor **3**, the bismacrocyclic ligands **6** and **7** were synthesized by the conjugation of 2.5 equiv of **3** with 1 equiv of DTPA-bisanhydride and EDTA-bisanhydride, respectively, in dry DMF and purified by preparative RP-HPLC. Finally, ligands L^1 and L^3 were obtained in 55–70% yields by deprotection of the *tert*-butyl groups with neat TFA and purified by RP-HPLC (Scheme 2).

In a similar manner, ligand L^2 was synthesized in a four-step synthesis starting from **1**. Alkylation on **1** with *p*-nitrobenzylbromide gave *p*-nitrobenzyl-containing ligand **4**, and the corresponding *p*-aminobenzyl derivative **5** was

(30) Paull, B.; Haddad, P. R. *TrAC, Trends Anal. Chem.* **1999**, *18*, 107.
(31) Corsi, D. M.; Platas, C.; Van Bekkum, H.; Peters, J. A. *Magn. Reson. Chem.* **2001**, *39*, 723.
(32) Mishra, A. K.; Chatal, J. F. *New J. Chem.* **2001**, *25*, 336.
(33) Duimstra, J. A.; Femia, F. J.; Meade, T. J. *J. Am. Chem. Soc.* **2005**, *127*, 12847.
(34) Mishra, A.; Pfeuffer, J.; Mishra, R.; Engelmann, J.; Mishra, A. K.; Ugurbil, K.; Logothetis, N. K. *Bioconjugate Chem.* **2006**, *17*, 773.
(35) Pope, S. J. A.; Kenwright, A. M.; Heath, S. L.; Faulkner, S. *Chem. Commun.* **2003**, *13*, 1550.
(36) Aime, S.; Cravotto, G.; Crich, S. G.; Giovenzana, G. B.; Ferrari, M.; Palmisano, G.; Sisti, M. *Tetrahedron Lett.* **2002**, *43*, 783.
(37) Wong, W.; Li, C. *PCT Int. Appl.* **2005**, 23.

Scheme 3. Synthesis of Ligand L^2 [a]

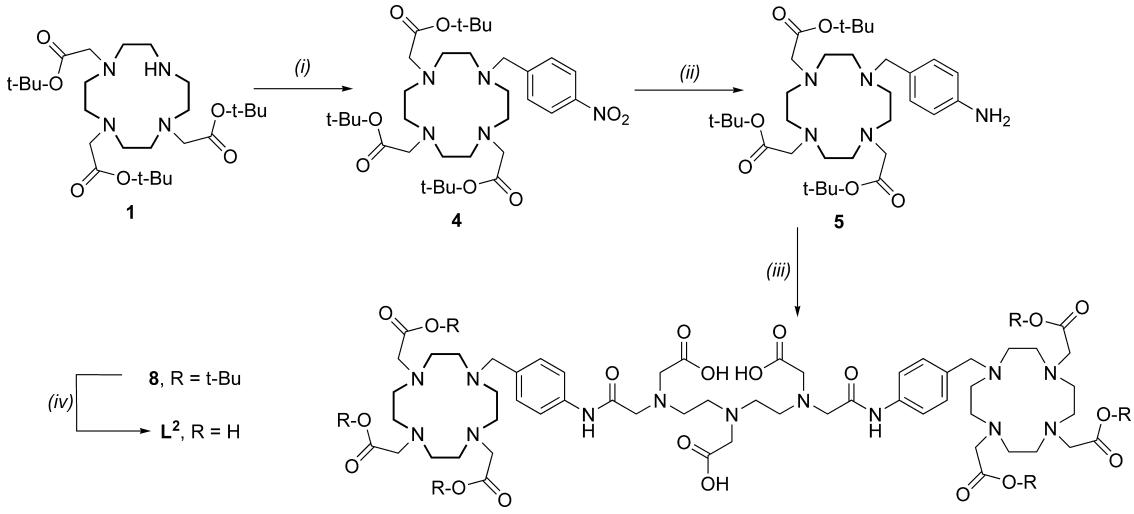

[a] Reagents and conditions: (i) 4-nitrobenzylbromide, MeCN, 82%; (ii) Pd/C (10%), H_2, MeOH, 90%; (iii) DTPA-bisanhydride, DMF, 42%; (iv) TFA, 55–60%.

obtained by the reduction of the nitro group in the presence of H_2, Pd/C (10%), and MeOH as a solvent in the Parr apparatus at room temperature.[38] The bismacrocyclic ligand **8** was synthesized by the conjugation of 2.5 equiv of **5** with 1 equiv of DTPA-bisanhydride in dry DMF and purified by preparative RP-HPLC. Finally, ligand L^2 was obtained in 60–65% yield by deprotection of the *tert*-butyl groups with TFA at room temperature and further purified by preparative RP-HPLC (Scheme 3).

Ln^{3+} complexes were synthesized with ligands L^1–L^3. ESI-MS for all complexes confirmed two lanthanide ions per bismacrocycle. In overall, we would like to emphasize that the present synthesis is facile and suitable for the straightforward preparation of potential 'smart' CAs.

Relaxometric Ca^{2+} Titrations of the Gd^{3+} Complexes. To investigate the sensitivity of the Gd^{3+} complexes toward Ca^{2+}, we measured the longitudinal relaxation times, T_1, of solvent–water protons as a function of the Ca^{2+} concentration. The relaxivity, r_1, was calculated for each Ca^{2+} concentration from eq 1.

$$\frac{1}{T_{1,\mathrm{obs}}} = \frac{1}{T_{1,\mathrm{d}}} + r_1[\mathrm{Gd}] \qquad (1)$$

where $T_{1,obs}$ is the observed longitudinal relaxation time, $T_{1,d}$ is the diamagnetic relaxation time in the absence of the paramagnetic substance, and [Gd] is the concentration of Gd^{3+}.

The titration curves were drawn by plotting the relaxivity as a function of the Ca^{2+}/Gd_2L molar ratio (Figure 1). The effect of Ca^{2+} on the relaxivity is different for the three complexes. For Gd_2L^1 and Gd_2L^3, the relaxivity increases by 15 and 32%, respectively, upon the addition of Ca^{2+}. On the other hand, Gd_2L^2 is practically insensitive toward Ca^{2+} (~6% relaxivity change). In this molecule, the Ca^{2+} binding site is separated by a rigid and sterically demanding benzene ring from the Gd^{3+} chelating unit, which renders the Gd^{3+}-containing moiety insensitive to Ca^{2+} coordination. For Gd_2L^1 and Gd_2L^3, the effect of Mg^{2+} has also been tested. For Gd_2L^1, the relaxivity increases with increasing Mg^{2+} concentration to reach a plateau at a slightly higher Mg^{2+}/Gd_2L^1 molar ratio than that observed with Ca^{2+}; however, the maximum relaxivity is identical in the two cases. By adding an additional 1.2 equiv of Ca^{2+} to this sample, no relaxivity change is observed. For Gd_2L^3, the relaxivity remains unchanged while adding an excess of Mg^{2+}. The relaxometric titration curves have been analyzed to obtain the association constants, K_A, for the Gd^{3+} complex–Ca^{2+} (or Mg^{2+}) interaction:

$$\mathrm{Gd_2L} + \mathrm{Ca} \rightleftarrows \mathrm{CaGd_2L} \text{ where } K_A = \frac{[\mathrm{CaGd_2L}]}{[\mathrm{Gd_2L}][\mathrm{Ca}]} \qquad (2)$$

The curves were fitted according to eq 3, where r_1^{obs} is the experimentally observed relaxivity, K_A is the association constant between the Gd^{3+} complex and Ca^{2+} or Mg^{2+}, c_{Gd_2L} and c_{Ca} are the total concentrations of the Gd^{3+} complex and the Ca^{2+}/Mg^{2+} ion, respectively, and r_1^0 and r_1^f are the initial and final relaxivities in the titration. In the fitting procedure, the association constant K_A and the initial and final relaxivities r_1^0 and r_1^f were the adjustable parameters. Similarly to previously investigated bismacrocyclic complexes,[10,20,39] a 1:1 binding stoichiometry was assumed.

$$r_1^{\mathrm{obs}} = \frac{(K_A c_{Gd_2L} + K_A c_{Ca} + 1) - \sqrt{(K_A c_{Gd_2L} + K_A c_{Ca} + 1)^2 - 4K_A^2 c_{Gd_2L} c_{Ca}}}{2K_A} - (r_1^f - r_1^0 + r_1^0 c_{Gd_2L}) \times 1000 \qquad (3)$$

The apparent association constants obtained from the fit are log K_A = 3.6 ± 0.1, 3.4 ± 0.1, and 2.7 ± 0.1 for the Gd_2L^1–Ca, Gd_2L^3–Ca, and Gd_2L^1–Mg systems, respectively. Ca^{2+} forms a less stable complex with Gd_2L^1 than with $DTPA^{5-}$ (the conditional stability constant of $CaDTPA^{3-}$ at

(38) Faulkner, S.; Pope, S. J. A. *J. Am. Chem. Soc.* **2003**, *125*, 10526.

(39) Dhingra, K.; Fousková, P.; Angelovski, G.; Maier, M. E.; Logothetis, N. K.; Tóth, É. *J. Biol. Inorg. Chem.* **2007**, *12*, 1.

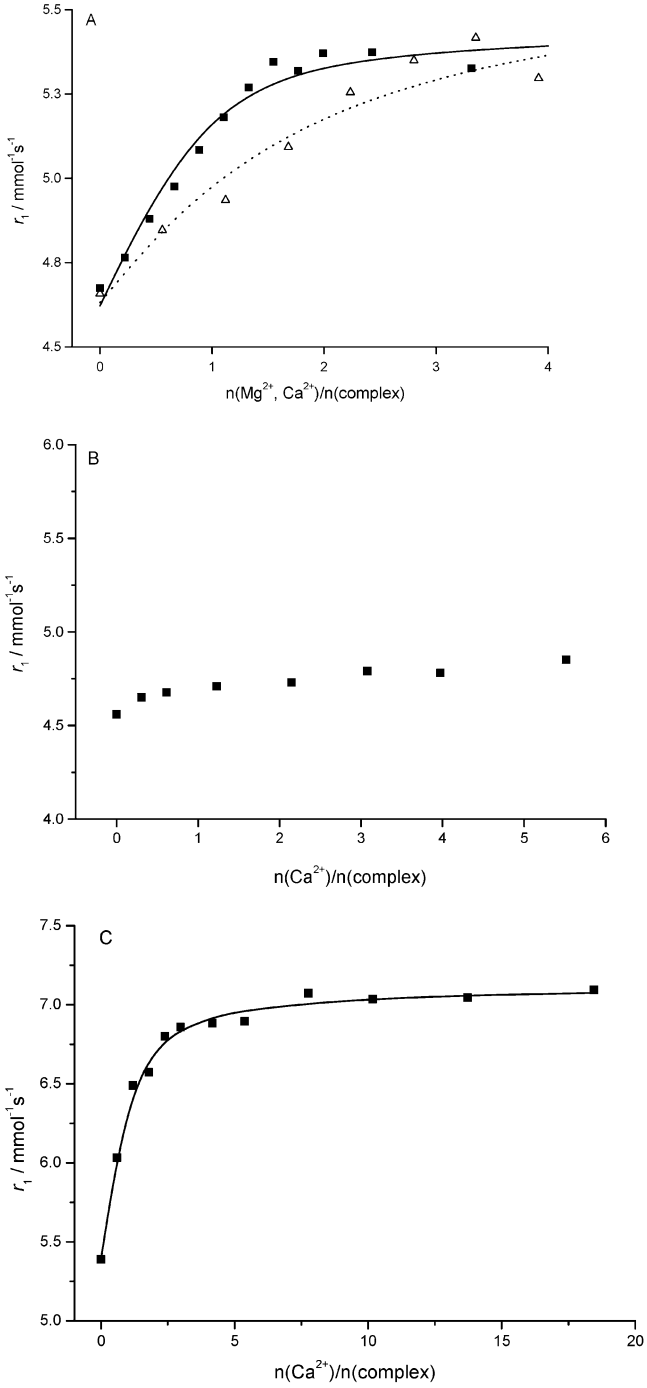

Figure 1. Relaxometric Ca^{2+} (full squares) and Mg^{2+} (empty triangles) titration curves of Gd_2L^1 (A), Gd_2L^2 (B), and Gd_2L^3 (C) performed at 25 °C and 11.75 T. The lines correspond to the fit as explained in the text.

pH 7.0 is log $K = 6.65$).[40] Such a decrease in stability can be expected, since in the central part of Gd_2L^1 only the three nitrogens and three carboxylates are coordinated to Ca^{2+}, in contrast to the three nitrogens and five carboxylates available in $DTPA^{5-}$. Indeed, the hydration numbers determined from the luminescence lifetime measurements on the corresponding Eu^{3+} complexes in the absence and presence of Ca^{2+} (see below) indicate that the amide function remains coordinated to the lanthanide even after Ca^{2+} binding. The association constant obtained for the Mg^{2+} adduct formed with Gd_2L^1 is slightly lower than that with Ca^{2+}, in accordance with the general tendency of Mg^{2+} to form less stable complexes than Ca^{2+}. Nevertheless, the selectivity of the DTPA-bisamide unit toward Ca^{2+} versus Mg^{2+} is much less important than that of $BAPTA^{4-}$ (selectivity over 10^5), a ligand which was specifically designed for Ca^{2+} complexation.[24] The value of the association constant calculated for Gd_2L^3 is also considerably lower than the conditional stability constant of $CaEDTA^{2-}$ at pH 7.0 (log $K = 7.79$).[40]

Table 1. Experimentally Measured Luminescence Lifetimes and Calculated Hydration Numbers of the Eu^{3+} Complexes, and Relaxivity Values (25 °C, 500 MHz) of the Gd^{3+} Analogues

complex	τ_{H2O} [ms]	τ_{D2O} [ms]	q	r_1 [mmol^{-1}s^{-1}]
Eu_2L^1	0.60	1.59	0.9	4.7
Eu_2L^1 with 2 equiv Ca^{2+}	0.62	1.57	0.9	5.4
Eu_2L^2	0.51	0.91	0.7	4.6
Eu_2L^3	0.54	1.84	1.3	5.4
Eu_2L^3 with 5 equiv Ca^{2+}	0.47	1.62	1.5	7.1

Luminescence and High Resolution UV–Vis Absorption Studies To Assess the Hydration State of the Eu^{3+} Complexes. In order to gain more insight into the factors that are responsible on the molecular level for the Ca^{2+}-dependent relaxivity change of Gd_2L^1 and Gd_2L^3, first of all, we have assessed the hydration state of the corresponding Eu^{3+} complexes before and after Ca^{2+} addition. The number of water molecules directly coordinated to Gd^{3+} is one of the fundamental parameters influencing the relaxivity. One of the widely used methods for the determination of the hydration number is to measure the luminescence lifetime decays on the corresponding europium(III) complexes.[41–43] This technique is based on relating the difference in luminescence lifetimes measured in H_2O and D_2O solutions to the hydration number. Hydration numbers were determined for Eu_2L^1, Eu_2L^2, and Eu_2L^3 complexes in the absence of and for Eu_2L^1 and Eu_2L^3 in the presence of 2 and 5 equiv of Ca^{2+}, respectively. These Ca^{2+}/Ln_2L complex ratios correspond to the saturation of the relaxometric titration curves obtained for the Gd^{3+} complexes. The hydration numbers were calculated according to the revised equation of Beeby et al.[43] (eq 4):

$$q = A'(\Delta k_{H_2} - k_{D_2})_{corr} \quad (4)$$

where A' is 1.2 ms and the correction factor for the contribution of the second and outer sphere water molecules is -0.25 ms^{-1}. The experimental luminescence lifetimes measured in H_2O and D_2O solutions and the corresponding hydration numbers q are listed in Table 1.

The noninteger numbers of q often imply the coexistence of differently hydrated species which can be investigated by high-resolution UV–vis measurements on the Eu^{3+} complexes. The Eu^{3+} ion has an absorption band in the visible

(40) Powell, K. J. *The IUPAC Stability Constants Database, SC-Database*; Academic Software: Yorks, U.K., 1999. http://www.acadsoft.co.uk (accessed Oct 2007).

(41) De, W.; Horrocks, W., Jr.; Sudnick, D. R. *J. Am. Chem. Soc.* **1979**, *101*, 334.

(42) Supkowski, R. M.; De, W.; Horrocks, W., Jr *Inorg. Chim. Acta* **2002**, *340*, 44.

(43) Beeby, A.; Clarkson, I. M.; Dickins, R. S.; Faulkner, S.; Parker, D. *J. Chem. Soc., Perkin Trans.* **1999**, *2*, 493.

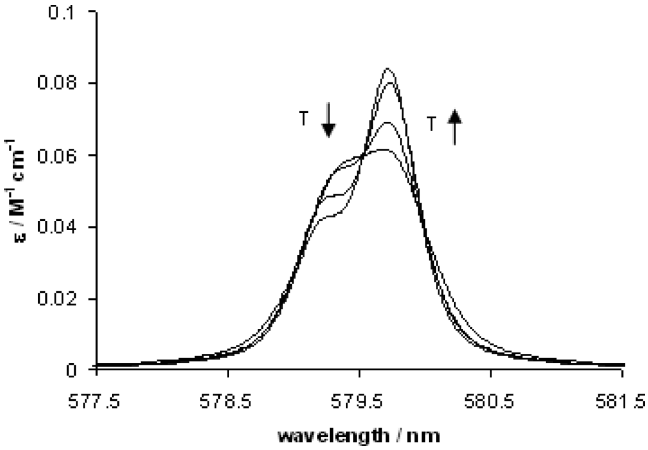

Figure 2. Representative UV–vis spectra of Eu_2L^2 (T = 92, 44, 16, and 5 °C).

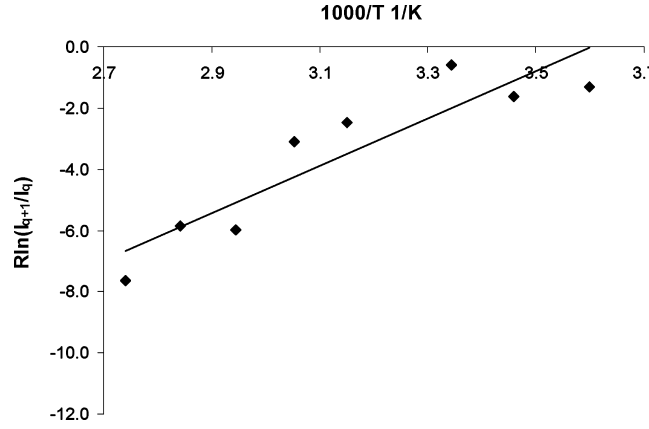

Figure 3. Ratio of the integrals of the two absorption bands attributed to $q = 0$ and $q = 1$ species in the UV–vis spectrum of Eu_2L^2 as a function of the inverse temperature. The straight line represents the linear least-squares fit to the data points as explained in the text.

spectrum (578–582 nm) whose wavelength is very sensitive to even small changes in the coordination environment. Although the intensity of this $^7F_0 \rightarrow {}^5D_0$ transition is low, the bands are relatively narrow, which allows distinguishing different coordination states of the metal. This transition has been previously used to determine the number of species present in solution,[44] and, in particular, to characterize hydration equilibria for Eu^{3+} complexes.[25,45–47] For Eu^{3+} complexes which have two differently hydrated forms in aqueous solution, one observes two absorption bands belonging to the two species.

High-resolution UV–visible spectra were recorded in aqueous solutions of Eu_2L^1, Eu_2L^2, and Eu_2L^3 complexes. In the region of the $^5D_0 \leftarrow {}^7F_0$ transition, the spectra of Eu_2L^1 and Eu_2L^3 show a temperature invariant absorption peak with a shoulder (see Supporting Information), while the spectrum of Eu_2L^2 has two distinct, temperature-dependent absorption bands (Figure 2). The intensity ratio of these two bands changes with temperature: the band at shorter wavelengths is decreasing, while that at longer wavelengths is increasing with the temperature. By analogy to previously studied systems,[45–47] we relate this temperature dependency to the existence of a hydration equilibrium. The band at lower energy (579.7 nm) is assigned to the nonhydrated, while that at ca. 579.2 nm is attributed to a monohydrated species (eq 5).

$$Eu_2L^2 + 2H_2O \rightleftarrows Eu_2(H_2O)_2L^2 \tag{5}$$

As the effective concentration of the solvent is constant, the equilibrium constant corresponding to eq 5 may be written as

$$K_{Eu} = \frac{[Eu_2(H_2O)_2L^2]}{[Eu_2L^2]} \tag{6}$$

The reaction enthalpy, ΔH^0, and the reaction entropy, ΔS^0, for the equilibrium may be obtained from the temperature dependence of K_{Eu}:

$$\ln K_{Eu} = \frac{\Delta S^0}{R} - \frac{\Delta H^0}{RT} \tag{7}$$

The ratio of the integrals of the two bands is related to the equilibrium constant, and its temperature dependence yields the reaction enthalpy and entropy (Figure 3). The fit of the data in Figure 3 to eq 8 resulted in $\Delta H^0 = -(7.8 \pm 1)$ kJ mol^{-1}, $\Delta S^0 = -(25 \pm 5)$ J mol^{-1} K^{-1}, and $K_{Eu}^{298} = (1.2 \pm 0.3)$.

$$\ln\left(\frac{\mathrm{Int}_q}{\mathrm{Int}_{q+1}}\right) = -\frac{\Delta H^0}{RT} + \frac{\Delta S^0}{R} + \ln\left(\frac{I_q}{I_{q+1}}\right) \tag{8}$$

The average hydration number derived from the equilibrium constant is 0.55 at 298 K, in acceptable accordance with $q = 0.7$ obtained from the luminescence decay measurements. If we assume that the overall coordination number of the lanthanide ion can be either 8 or 9, it implies that in both the nonhydrated (CN = 8) and monohydrated (CN = 9) species another donor atom from the central part of the ligand (an amide or a carboxylate oxygen) completes the coordination sphere. Given the important steric demand and rigidity that the benzyl group represents, this scenario seems rather unlikely. Moreover, the Ca^{2+} independency of the relaxivities for the Gd_2L^2 complex indicates that Ca^{2+} binding has no effect on the hydration state of the lanthanide ion. This would mean that, if a donor group is bound to the lanthanide ion from the central part of the molecule, it will remain coordinated even after Ca^{2+} binding. The other, likely more probable coordination mode involves the binding of the macrocycle amines and carboxylates to the lanthanide, plus one water molecule in the monohydrated species. The bulky and highly hydrophobic benzyl group directly attached to the amine nitrogen prevents the coordination of another donor atom; thus, in this case, the coordination equilibrium observed in the UV–vis spectrum would correspond to nonhydrated CN = 7 and monohydrated CN = 8 species. This hypothesis seems to be also supported by the high negative value of the activation entropy, $\Delta S^{\ddagger}$, calculated

(44) Albin, M.; Farber, G. K.; Horrocks, W. D., Jr *Inorg. Chem.* **1984**, *23*, 1648.
(45) Geier, G.; Jorgensen, C. K. *Chem. Phys. Lett.* **1971**, 263.
(46) Tóth, É.; Ni Dhubhghaill, O. M.; Besson, G.; Helm, L.; Merbach, A. E. *Magn. Reson. Chem.* **1999**, *37*, 701.
(47) Yerly, F.; Dunand, F. A.; Tóth, É.; Figueirinha, A.; Kovács, Z.; Sherry, A. D.; Geraldes, C. F. G. C.; Merbach, A. E. *Eur. J. Inorg. Chem.* **2000**, 1001.

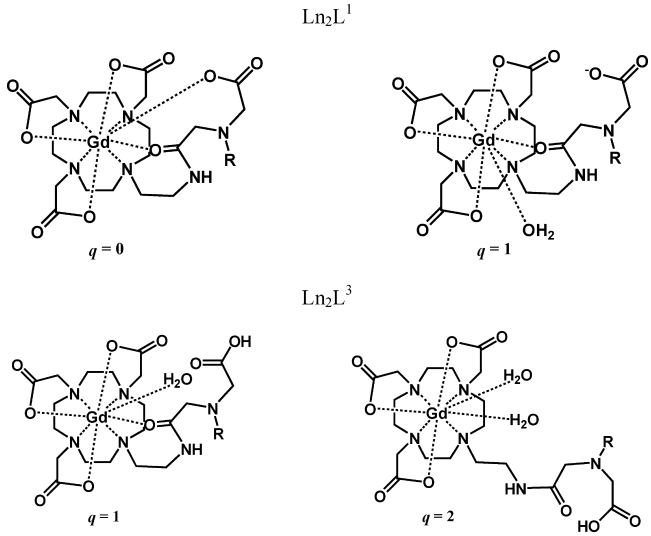

Figure 4. Proposed structures present in solutions of Ln_2L^1 and Ln_2L^3. In both cases, Ca^{2+} binding in the central part of the bismacrocycle favours the presence of the more hydrated species. R stands for the remaining part of the bismacrocyclic complex.

for the water exchange on Gd_2L^2 (see below), indicative of the associative activation mode of the exchange process. This is in contrast to the nine-coordinated Gd^{3+} poly(aminocarboxylate) complexes which have, in a great majority of the cases, a dissociatively activated water exchange.[48]

The temperature invariance of the UV–vis spectrum for Eu_2L^1 and Eu_2L^3 suggests that no hydration equilibrium exists in the sense as depicted for Eu_2L^2. Nevertheless, the presence of a shoulder next to the main band in the $^7F_0 \rightarrow {}^5D_0$ transition range implies that there are at least two different coordination environments. By taking into account all available experimental information from luminescence, UV–vis absorption, and relaxivity data, we can hypothesize the existence of two species as depicted in Figure 4. In all cases, the macrocyclic carboxylates and nitrogens are coordinated to the lanthanide(III) ion. The inner coordination sphere is then completed in different manners: in Ln_2L^1, we expect the coordination of the amide oxygen, while the ninth coordination site can be occupied either by a water molecule or by one of the central carboxylates. This hypothesis is in accordance with the hydration number of $q = 0.9$ determined by luminescence. It also explains the increase of the relaxivity of the Gd^{3+} complex on Ca^{2+} coordination in the central part of the ligand which will involve the carboxylate, coordinated to the lanthanide in the absence of Ca^{2+}. We expect that on Ca^{2+} binding this carboxylate is replaced by an inner-sphere water molecule, leading to the relaxivity increase observed for Gd_2L^1. The luminescence lifetime measurements do not indicate a change in q on Ca^{2+} addition (Table 1); however, the uncertainty generally associated with the q values determined by this method is at least ± 0.25 (certain authors estimate this uncertainty as high as ± 0.5).[43] By taking this into consideration, the luminescence measurements do not confute our hypothesis. An analogous scenario has been previously proposed for bismacrocyclic GdDO3A complexes with a BAPTA-bisamide central bridging unit.[39]

For Ln_2L^3, we suggest that, in addition to the macrocycle nitrogens and carboxylates, the first coordination sphere of the lanthanide ion is completed by two water molecules in one species and one water and one amide in another species. It is supported by the hydration number $q = 1.3$ obtained for Eu_2L^3 by luminescence. On the other hand, the increase of q and of the relaxivity observed on Ca^{2+} addition evidence the transfer of a donor group (the amide) from Ln^{3+} to Ca^{2+}. The detachment of this amide from the Gd^{3+} then results in the entering of a second inner-sphere water. The higher hydration number determined for Ln_2L^3 as compared to Ln_2L^1 is also consistent with the respective structure of the two complexes: the shorter bridging unit in the EDTA-bisamide derivative bismacrocycle implies more steric constraint, which then prevents the simultaneous coordination of the amide and a central carboxylate to the lanthanide ion, leading to a higher q. In contrast, such a coordination mode involving the carboxylate of the central part is more accessible in Ln_2L^1, which possesses a longer, thus more flexible, DTPA-bisamide bridging unit. For both Ln_2L^1 and Ln_2L^3, the overall coordination number is CN = 9 before and after Ca^{2+} addition.

Evaluation of the Parameters Influencing Relaxivity of the Gd^{3+} Complexes. For all three of the systems, variable-temperature ^{17}O NMR and ^1H NMRD relaxometric data have been acquired and analyzed simultaneously on the basis of the Solomon–Bloembergen–Morgan approach. The experimentally measured paramagnetic ^{17}O chemical shifts were considerably smaller than what would be expected for a Gd^{3+} complex with the given q value; therefore, they have not been included in the final fitting. A similar diminution of the chemical shifts has been previously reported in systems with a significant second-sphere contribution to ^{17}O and ^1H relaxation.[39,49,50] An important second-sphere effect has been proved to exist for bismacrocyclic Gd^{3+} complexes of analogous structure.[20,39] Therefore, the common Solomon–Bloembergen–Morgan model was extended with a second-sphere contribution to proton relaxivity,[51] as has been done for other systems.[52–56] Certain of the large number of parameters were fixed in the fit.[57] Namely, the number of inner-sphere water molecules (q) was fixed to the values

(48) Helm, L.; Merbach, A. E. *Chem. Rev.* **2005**, *105*, 1923.
(49) Lebdušková, P.; Hermann, P.; Helm, L.; Tóth, É.; Kotek, J.; Binnemans, K.; Rudovský, J.; Lukeš, I.; Merbach, A. E. *Dalton Trans.* **2007**, 493.
(50) Lebdušková, P.; Sour, A.; Helm, L.; Tóth, É.; Kotek, J.; Lukeš, I.; Merbach, A. E. *Dalton Trans.* **2006**, 3399.
(51) Botta, M. *Eur. J. Inorg. Chem.* **2000**, 399.
(52) Rudovský, J.; Cígler, P.; Kotek, J.; Hermann, P.; Vojtíšek, P.; Lukeš, I.; Peters, J. A.; Vander Elst, L.; Muller, R. N. *Chem.—Eur. J.* **2005**, *11*, 2373.
(53) Rudovský, J.; Kotek, J.; Hermann, P.; Lukeš, I.; Mainero, V.; Aime, S. *Org. Biomol. Chem.* **2005**, *3*, 112.
(54) Rudovský, J.; Botta, M.; Hermann, P.; Koridze, A.; Aime, S. *Dalton Trans.* **2006**, 2323.
(55) Kotek, J.; Lebdušková, P.; Hermann, P.; Vander Elst, L.; Muller, R. N.; Maschmeyer, T.; Lukeš, I.; Peters, J. A. *Chem.—Eur. J.* **2003**, *9*, 5899.
(56) Lebdušková, P.; Kotek, J.; Hermann, P.; Vander Elst, L.; Muller, R. N.; Lukeš, I.; Peters, J. A. *Bioconjugate Chem.* **2004**, *15*, 881.
(57) Powell, D. H.; Dhubhghaill, O. M. N.; Pubanz, D.; Helm, L.; Lebedev, Y. S.; Schlaepfer, W.; Merbach, A. E. *J. Am. Chem. Soc.* **1996**, *118*, 9333.

Table 2. Best-Fit Parameters Obtained by the Simultaneous Analysis of Transverse ^{17}O Relaxation Rates and Proton Relaxivities for Gd_2L^1, Gd_2L^2, and Gd_2L^3 Complexes in the Absence of Ca^{2+} [a]

parameter	Gd_2L^1	Gd_2L^2	Gd_2L^3	GdDOTA[b]
r_1 [mmol^{-1} s^{-1}] 20 MHz/37 °C	6.22	8.19	6.05	3.83
k_{ex}^{298} [10^6 s^{-1}]	0.52 ± 0.06	0.8 ± 0.1	80 ± 20	4.1
$\Delta H^{\ddagger}$ [kJ mol^{-1}]	39.3 ± 1.4	20.1 ± 2.2	20 ± 4	49.8
$\Delta S^{\ddagger}$ [J mol^{-1} K^{-1}]	−3.6 ± 4.2	−64.5 ± 6.6	−27 ± 12	+49
τ_{RH}^{298} [ps]	390 ± 8 450 ± 10[c]	1060 ± 210	200 ± 25	77
E_R [kJ mol^{-1}]	30 ± 6 30 ± 5[c]	30 ± 4	24 ± 7	16.1
τ_V^{298} [ps]	20.6 ± 1.1	25.0 ± 0.9	21 ± 31	11
Δ^2 [10^{20} s^{-2}]	0.43 ± 0.03	0.26 ± 0.02	0.6 ± 0.1	0.16
D_{GdH}^{298} [10^{-10} m^2 s^{-1}]	28 ± 2	21 ± 1	25 ± 8	22
E_{DGdH} [kJ mol^{-1}]	19 ± 2	18 ± 3	25 ± 9	20
q[d]	*0.9* 1.1 ± 0.1[c]	*0.5*[e]	*1.3*	1
q^{second}	*1*	*1*	*1*	

[a] Parameters obtained from the fit of NMRD data for Gd_2L^1 in the presence of Ca^{2+} are also presented. Values in *italics* were fixed during the fit. [b] From ref 57. [c] From fitting the NMRD curves in the presence of Ca^{2+}. The parameters describing water exchange, electron spin relaxation, and second and outer sphere relaxation were fixed to the values obtained without Ca^{2+}. [d] Obtained from luminescence data on the Eu^{3+} complex. [e] At 298 K; in the fit, q was calculated for each temperature from the UV–vis measurements on the Eu^{3+} complex.

found from luminescence lifetime measurements (0.9 and 1.3 for Gd_2L^1 and Gd_2L^3, respectively). For Gd_2L^2, the actual q value was calculated for each temperature by using the reaction enthalpy and entropy of the hydration equilibrium as determined for the Eu^{3+} analogue from the variable-temperature UV–vis study. The distance of Gd^{3+} from the water proton (r_{GdH}) was fixed to 3.1 Å; the distance of the closest approach of the outer-sphere water molecules to Gd^{3+} (a) was fixed to 3.6 Å. The hyperfine coupling constant ($A/\hbar$) was set to -3.8×10^6 rad·s^{-1}, a value found previously for GdDOTA.[57] The activation energy E_V had to be fixed to 1 kJ·mol^{-1}; otherwise, the fit converged to negative values. Parameters related to the second hydration sphere were fixed to the following values:[49,50,58,59] the number of second-sphere water molecules (q^{second}) was set to 1, the Gd second-sphere proton distance (r_{GdH}^{second}) to 3.5 Å. The residence time of the second-sphere water (τ_m^{second}) was set to 50 ps and its enthalpy of activation to 35 kJ·mol^{-1}. The parameters leading to the best least-squares fits are listed in Table 2 and compared with the parent GdDOTA. The simultaneous fits are depicted in Figure 5.

With regard to the water exchange rate, the Gd_2L^1 and Gd_2L^2 complexes are considerably different from Gd_2L^3. The water exchange is remarkably fast on Gd_2L^3 ($k_{ex}^{298} = 8 \times 10^7$ s^{-1}), about 20 times faster than on GdDOTA. It is interesting to note that Congreve et al. reported a similarly fast water exchange ($k_{ex}^{298} = 11 \times 10^7$ s^{-1}) for the Gd^{3+} complex of a DO3A ligand bearing an N-linked CH_2–CH_2NHCO–pyridyl moiety.[60] For the Eu^{3+} analogue of this chelate, they found $q = 1.1$ by luminescence, a slightly lower value than $q = 1.3$ for Eu_2L^3. They interpreted the unexpectedly fast water exchange in terms of a steric destabilization of the Ln–water binding interaction by the coordination of the sterically demanding N-linked amide. The same explanation can be evoked in the case of Gd_2L^3. We should also note that the Gd_2L^3 complex is present in an aqueous solution as a mixture of two differently hydrated species. Consequently, the water exchange rate calculated here represents an effective value which we cannot decompose to the individual k_{ex} values corresponding to each of the two species.

In contrast to Gd_2L^3, in Gd_2L^1, the participation of a central carboxylate in the Gd^{3+} coordination creates a different coordination environment with less than one inner-sphere water on average and results in a low exchange rate ($k_{ex}^{298} = 0.5 \times 10^6$ s^{-1}). A k_{ex}^{298} value on the same order of magnitude ($k_{ex}^{298} = 2.4 \times 10^6$ s^{-1}) was found for the bismacrocyclic GdDO3A complex with a BAPTA-bisamide central unit.[39]

The rotational correlation time, τ_R, is influenced by the size and the rigidity of the complex. All three systems studied have a higher molecular weight and therefore higher τ_R than GdDOTA, which is also reflected in the higher relaxivities. We note the remarkably high relaxivity of Gd_2L^2, which is the most rigid among the three complexes due to the presence of the benzyl groups and, accordingly, has the highest τ_R. In all cases, we also expect an influence of the second-sphere water on the overall relaxivity induced by the negatively charged carboxylate groups in the central part of the molecules.

The simultaneous fit of the ^1H and ^{17}O relaxation rates also supplies parameters that describe the electron-spin relaxation of the Gd^{3+} complexes, such as τ_v, the correlation time for the modulation of the zero field splitting, its activation energy, E_v, and the mean zero field splitting energy, Δ^2. The values obtained for the Gd_2L complexes are in the usual range for similar systems.[57]

The relaxivity of Gd_2L^2 is practically invariant upon Ca^{2+} addition (Figure 1B). Concerning the Ca^{2+}-dependent systems, transverse ^{17}O relaxation rates (for Gd_2L^1 and Gd_2L^3) and ^1H NMRD profiles (for Gd_2L^1) have been measured in the presence of 3 and 4 equiv of Ca^{2+}, respectively. For both complexes, the ^{17}O $\ln(1/T_{2r})$ data were identical with those obtained in the absence of Ca^{2+} (see the Supporting Information); that is, the water exchange rate is not affected by the presence of Ca^{2+}. The NMRD profiles of Gd_2L^1 in the presence of Ca^{2+} have been fitted to the Solomon–Bloembergen–Morgan theory by calculating the rotational correlation time and its activation energy and fixing the other parameters to the values found for the Ca^{2+}-free system (Figure S5 in the Supporting Information). We assumed one water molecule in the second sphere, as for the Ca^{2+}-free complex. The Ca^{2+} binding might change the second-sphere contribution, since this cation will occupy the free donor atoms of the central moiety, which, in the absence of Ca^{2+}, are supposed to be the main sites for hydrogen bonding for second-sphere water. However, it is very difficult to estimate to what extent the second-sphere contribution is affected by

(58) Rudovský, J.; Hermann, P.; Botta, M.; Aime, S.; Lukeš, I. *Chem. Commun.* **2005**, 2390.
(59) Rudovský, J.; Botta, M.; Hermann, P.; Hardcastle, K. I.; Lukeš, I.; Aime, S. *Bioconjugate Chem.* **2006**, *17*, 975.
(60) Congreve, A.; Parker, D.; Gianolio, E.; Botta, M. *Dalton Trans.* **2004**, 1441.

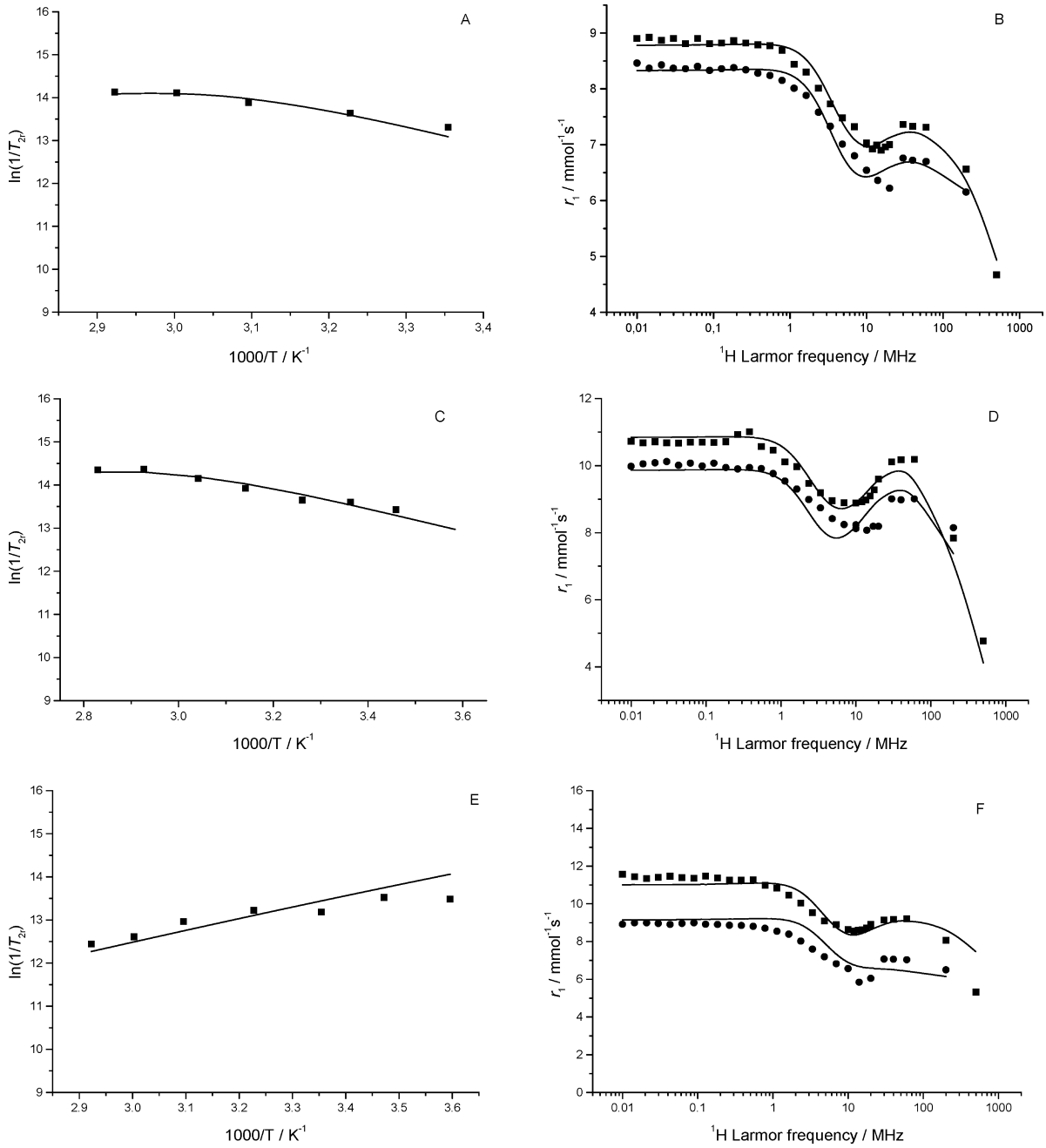

Figure 5. Simultaneous fitting of ^{17}O $\ln(1/T_{2r})$ (■) and ^{1}H NMRD (25 °C ■, 37 °C ●) data for Gd_2L^1 (A, B), Gd_2L^2 (C, D), and Gd_2L^3 (E, F), in the absence of Ca^{2+}.

Ca^{2+} binding; therefore, we preferred to use the same contribution in both cases. By fixing the hydration number to the value determined by luminescence, no acceptable fit of the NMRD curves could be obtained. Therefore, q was also adjusted in the final fit. The value calculated in this way, $q = 1.1$, is slightly higher than that determined by luminescence (0.9). The rotational correlation time is also increased when Ca^{2+} is bound in the central part of the molecule ($\tau_R^{298} = 390$ and 450 ps before and after Ca^{2+} binding, respectively). Overall, the relaxivity increase observed upon Ca^{2+} addition is mainly due to the increase of the hydration number of the Gd^{3+}. In addition, Ca^{2+} binding also leads to a slightly more important rigidity of the entire molecule, resulting in a longer rotational correlation time, τ_R.

Li et al. reported a mechanistic study to assess the parameters that are responsible for the Ca^{2+}-dependent relaxivity variation of GdDOPTA, a bismacrocyclic chelate possessing a Ca^{2+}-binding $BAPTA^{4-}$ unit as bridging part between the two macrocycles.[20] They considered that the rotational correlation time does not vary upon Ca^{2+} binding. We think that the binding of the Ca^{2+} will render the molecule more rigid, as is indeed reflected by the increase of the rotational correlation time calculated from the NMRD data. On the other hand, for GdDOPTA, a more important variation of q was reported on Ca^{2+} coordination. By luminescence on the Tb^{3+} analogue, a hydration number of $q = 0.47$ and 1.05 was determined before and after Ca^{2+} binding; for the Gd^{3+} complex, the fit of the NMRD profiles

suggested $q = 0.7$ and 2.3 without and with Ca^{2+}, respectively. The relaxivity increase was also more significant (~80% at 500 MHz) for GdDOPTA and was not sensitive to the presence of Mg^{2+}.

Due to the high association constant between the BAPTA^{4-} chelator and Ca^{2+} ($K_a \sim 10^6$ M^{-1}), GdDOPTA might be adapted to report on the variation of Ca^{2+} concentration at the micromolar level (intracellular), but its relaxivity response will be leveled off at higher Ca^{2+} concentrations, such as those in the extracellular space (millimolar range). In order to probe variations at the millimolar level, the association constant should be decreased, as is the case for our compounds. Unfortunately, the DTPA-bisamides do not have the great selectivity of BAPTA^{4-} for Ca^{2+} with respect to Mg^{2+}, which prevents practical application of this compound for Ca^{2+} sensing. The EDTA-bisamide is more selective toward Ca^{2+}; therefore, Gd_2L^3 can be useful for further *in vitro* or *in vivo* Ca^{2+}-sensing studies.

Conclusion

In this work, we report the straightforward synthesis of three novel bismacrocyclic DO3A-type ligands: L^1, L^2, and L^3. They have a DTPA- or EDTA-bisamide moiety as the bridging part between the macrocycles, representing a potential Ca^{2+} binding site (Scheme 1). The sensitivity of their relaxivity toward Ca^{2+} largely depends on the structure of the ligand. Upon Ca^{2+} addition, the relaxivities of Gd_2L^1 and Gd_2L^3 increase by 15% and 32%, respectively, while Gd_2L^2 is practically insensitive to Ca^{2+} binding. Hydration numbers were determined from luminescence lifetime measurements on the corresponding Eu^{3+} complexes in the absence and presence of Ca^{2+}. High-resolution UV–vis spectra of the Eu^{3+} complexes of L^1, L^2, and L^3 show a band with a shoulder, indicating at least two different coordination environments. This was related to differently hydrated species, in agreement with the noninteger q values obtained by luminescence. When Ca^{2+} is coordinated in the central part of the ligand, a donor group is removed from the coordination sphere of the lanthanide ion and is replaced by a water molecule, which shifts the hydration equilibrium toward the more hydrated species.

Water exchange is relatively slow on Gd_2L^1 and Gd_2L^2, while it is ~2 orders of magnitude faster on Gd_2L^3; in all cases, it is insensitive to Ca^{2+} binding. Due to the benzene linker between the macrocycles and the central DTPA-bisamide unit, the Gd_2L^2 complex is particularly rigid and, hence, has a high relaxivity. A detailed analysis of the luminescence, ^{17}O NMR and NMRD data on the Eu^{3+} and Gd^{3+} complexes of L^1 and L^3 in the absence and presence of Ca^{2+}, proved that the relaxivity increase observed upon Ca^{2+} addition can be ascribed to the increase in the hydration number, q, and to the slight rigidification of the complex induced by Ca^{2+} binding.

Acknowledgment. We are grateful to Prof. Lothar Helm (Ecole Polytechnique Fédérale de Lausanne, Switzerland) for allowing us to use the relaxometric facilities. We thank Dr. Klaus Albert (University of Tübingen, Germany) for providing access to the analytical facilities. The authors also thank Prof. A. J. Meixner (University of Tübingen, Germany) for providing access to the fluorescence spectrometer and Dr. I. Mamedov (MPI for Biological Cybernetics, Tübingen, Germany) for his help with luminescence lifetime experiments. Financial support from the Max Planck Society and the Hertie Foundation is gratefully acknowledged. This work was carried out in the framework of the EC COST D38 Action and supported by the Ministère de l'Education Nationale et de la Recherche and the Centre National pour la Recherche Scientifique (France).

Note Added after Print Publication. Due to a production error, Figure 1 and its caption were omitted in the version posted on the Web January 1, 2008 (ASAP), and published in the February 18, 2008, issue (Vol. 47, No. 4, pp 1370–1381); the correct electronic version of the paper was published on March 28, 2008, and an Addition & Correction appears in the April 21, 2008, issue (Vol. 47, No. 8).

Supporting Information Available: Equations used in the analysis of ^{17}O NMR and ^1H NMRD data; proton relaxivities of Gd_2L^1, Gd_2L^2, and Gd_2L^3 in the absence and presence of Ca^{2+}; variable-temperature reduced transverse ^{17}O relaxation rates of Gd_2L^1 in the absence and presence of Ca^{2+}; variable-temperature reduced transverse ^{17}O relaxation rates of Gd_2L^2 and Gd_2L^3 in the absence of Ca^{2+}; relaxometric Ca^{2+} titration data for Gd_2L^1, Gd_2L^2, and Gd_2L^3; luminescence lifetimes measurements on Eu_2L^1, Eu_2L^2, and Eu_2L^3; variable-temperature UV–vis spectra of Eu_2L^1, Eu_2L^2, and Eu_2L^3; ^{13}C NMR and ^1H NMR of the ligands (L^1–L^3); fit of NMRD data for Gd_2L^1 in the presence of 3 equiv of Ca^{2+}. This material is available free of charge via the Internet at http://pubs.acs.org.

IC7017456